ISSN 1064-2269, Journal of Communications Technology and Electronics, 2023, Vol. 68, No. 4, pp. 431–435. © Pleiades Publishing, Inc., 2023.
Russian Text © The Author(s), 2023, published in Radiotekhnika i Elektronika, 2023, Vol. 68, No. 4, pp. 372–377.

ON THE 90th ANNIVERSARY OF VLADIMIR GRIGOR'EVICH SHAVROV

Magnetic and Magnetocaloric Characteristics of the $Mn_{1.9}Cu_{0.1}Sb$ Alloy

V. I. Mitsiuk[a, *], A. V. Gurbanovich[a], A. V. Gurbanovich[a], T. M. Tkachenko[b], V. I. Valkov[c], A. V. Golovchan[c], A. V. Mashirov[d], and Z. Surowiec[e, f]

[a] *Scientific and Practical Center, National Academy of Sciences of Belarus for Materials Science, Minsk, 220072 Belarus*
[b] *Belarusian State Agrarian Technical University, Minsk, 220012 Belarus*
[c] *Donetsk Institute of Physics and Technology, Donetsk, 283050 Russia*
[d] *Institute of Radioengineering and Electronics, RAS, Moscow, 125009 Russian Federation*
[e] *Joint Institute for Nuclear Research, Moscow oblast, Dubna, 141980 Russia*
[f] *Institute of Physics, University Maria Curie-Sklodowska, Lublin, 20-031 Poland*
**e-mail: mitsiuk@physics.by*

Received September 13, 2022; revised October 7, 2022; accepted October 7, 2022

Abstract—The magnetic and magnetocaloric characteristics of the $Mn_{1.9}Cu_{0.1}Sb$ alloy were studied. The presence of a relatively sharp decrease in the magnetization in the region of 100 K is established, which, according to ab initio calculations, can be interpreted as antiferromagnetism–ferrimagnetism transitions. The presence of a magnetic phase transition from a ferrimagnetic to an antiferromagnetic state (F ↔ AF) leads to the appearance of an inverse magnetocaloric effect, which is preserved in magnetic fields up to 10 T.

DOI: 10.1134/S1064226923040095

INTRODUCTION

Recent active study of magnetic materials based on manganese pnictides has been stimulated by the wide variety of magnetic phase transformations found in them and, as a consequence, by the large value of the inverse magnetocaloric effect [1]. The latter makes it possible to significantly simplify the design of magnetic refrigerators and reduce heat losses on structural elements [2]. A promising system for magnetic cooling in the cryogenic temperature range is $Mn_{2-x}Cu_xSb$, in which an order–order transition is observed in the region of 100 K [3–6].

Objective—To study the structural, magnetic, and magnetocaloric characteristics of the $Mn_{1.9}Cu_{0.1}Sb$ alloy.

1. RESULTS AND DISCUSSION

To study the magnetocaloric properties of this system, at the first stage, we synthesized a sample of $Mn_{1.9}Cu_{0.1}Sb$ and its magnetic properties were measured. The basis of the technology for obtaining solid solutions of $Mn_{2-x}Me_xSb$ (*Me* – Zn, Cu) with a Cu_2Sb type structure was used for the previously tested technology for obtaining zinc-containing manganese pnictides [7], which was optimized in the course of work for the objects under study. A sample of $Mn_{1.9}Cu_{0.1}Sb$ was obtained by direct fusion of finely dispersed manganese, copper, and antimony powders taken in the required calculated amounts and carefully mixed. The phase composition and unit cell parameters were determined at room temperature by X-ray diffraction analysis using CuK_α-radiation. To determine the isothermal change in entropy in the region of the phase transition, measurements of the magnetization in static fields up to 10 T were carried out. The magnetocaloric characteristics were calculated by an indirect method based on Maxwell's thermodynamic relations.

As a result of X-ray diffraction studies of the synthesized sample, it was found that the $Mn_{1.9}Cu_{0.1}Sb$ alloy has a tetragonal crystal structure similar to Cu_2Sb (symmetry group $P4/nm$) with crystal lattice parameters a = 4.078 Å and c = 6.539 Å. The X-ray diffraction pattern of $Mn_{1.9}Cu_{0.1}Sb$ alloy obtained at room temperature in the angle range $20° \le 2\Theta \le 90°$ is shown in Fig. 1.

X-ray phase analysis showed that the $Mn_{1.9}Cu_{0.1}Sb$ alloy is not strictly single-phase, it contains a small amount (≈5–7%) of the hexagonal nickel-arsenide phase. It is known [8] that in the matrix Mn_2Sb always contains nuclei of the MnSb phase, which is also characteristic of the $Mn_{1.9}Cu_{0.1}Sb$ sample, close in composition to Mn_2Sb. It can be seen that, in the X-ray dif-

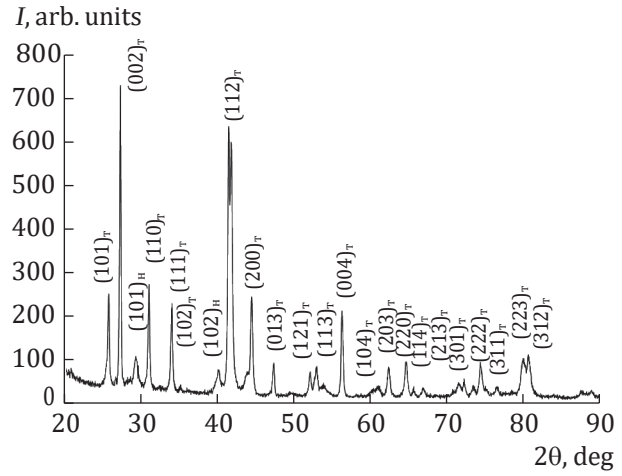

Fig. 1. X-ray diffraction pattern of $Mn_{1.9}Cu_{0.1}Sb$ alloy.

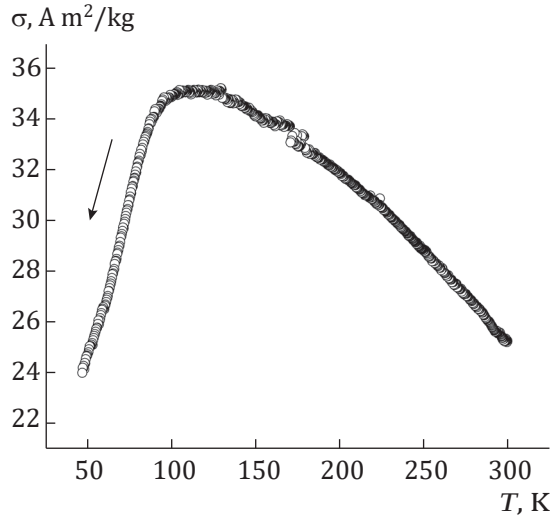

Fig. 2. Temperature dependence of the magnetization of the $Mn_{1.9}Cu_{0.1}Sb$ alloy in a magnetic field of 1 T during cooling.

fraction pattern of the alloy at room temperature (see Fig. 1), along with the reflections of the main tetragonal phase, there are reflections of the hexagonal phase of low intensity.

The results of measurements of the specific magnetization of the studied compositions are shown in Fig. 2. Magnetic measurements were carried out on polycrystalline samples using the inductive method on a vibrating magnetometer from Cryogenic Limited.

As can be seen from Fig. 2, upon cooling below 100 K, the magnetization of the sample decreases, which, according to the literature data on magnetic phase transitions in Mn_2Sb-based alloys [16] corresponds to a phase transition from a ferrimagnetic to an antiferromagnetic state (F ↔ AF). Such order-to-order transitions are often accompanied by an inverse magnetocaloric effect [9].

The electronic structure and interatomic exchange integrals were calculated by the fully relativistic Korringa–Kohn–Rostoker method (SPRKKR v8.6 package [10, 11]) in the coherent potential approximation (KKR–CPA) for a disordered alloy. For the crystal potential, the approximation of atomic spheres was used. For the exchange-correlation energy, an approximation was chosen that gives the best agreement between the calculated magnetic moments and the experimental ones. The local density approximation [12] was used without taking into account gradient corrections. The interatomic exchange integrals were calculated according to the procedure [13] based on the calculation of the variation of the total energy functional with respect to the deviation of a chosen pair of spins from the equilibrium position. The lattice parameters are determined from the data of X-ray diffraction analysis (a = 4.078 Å, c = 6.539 Å). In the structure under study, Mn atoms occupy positions of the type 2a(0, 0, 0) and 2c(1/4, 1/4, z_1), Sb atoms are positions of type 2c(1/4, 1/4, z_2) space group $P4/nm$. Position parameters z_1 = 0.2897 and z_2 = 0.7207 correspond to the structure of pure Mn_2Sb. The Cu atoms were assumed to be uniformly distributed over the Mn positions. Four types of magnetic structures were considered: ferromagnetic (FM), ferrimagnetic (FIM), and two antiferromagnetic (AF1, AF2). The orientation of the magnetic moments of manganese in the AF1 structure corresponds to the antiferromagnetic structure Mn_2As (magnetic moments of Mn atoms$_I$ and Mn$_{II}$ from neighboring layers are directed oppositely), and the AF2 structure corresponds to the antiferromagnetic structure of Fe_2As (magnetic moments of Mn$_I$ and Mn$_{II}$ atoms from neighboring layers are codirectional) [14]. According to the calculation data, FIM(–70727.47111598Ry) has the lowest energy, followed by FM(–70727.46506323 Ry), AF1(–70727.46152557 Ry), and AF2(–70727.41038789 Ry). The magnetic moments of manganese atoms are M(Mn$_I$) = 3.2μ_B, M(Mn$_{II}$) = 3.76μ_B and vary by 0.1–0.3μ_B in magnitude as the orientation changes. The magnetic moments of copper and antimony atoms do not exceed 0.2μ_B.

The electronic structure of $Mn_{1.9}Cu_{0.1}Sb$ is shown in Fig. 3 for FIM and AF1 structures. The spin-polarized density of electronic states has a typical multipeak structure characteristic of 3d-metal compounds. The main contribution to the formation of the magnetic and transport properties is made by the d-electrons of manganese. A comparison of the partial densities of electronic states of manganese atoms in the FIM and AF1 structures indicates a significant change in the behavior of the density of states of Mn$_I$ in the

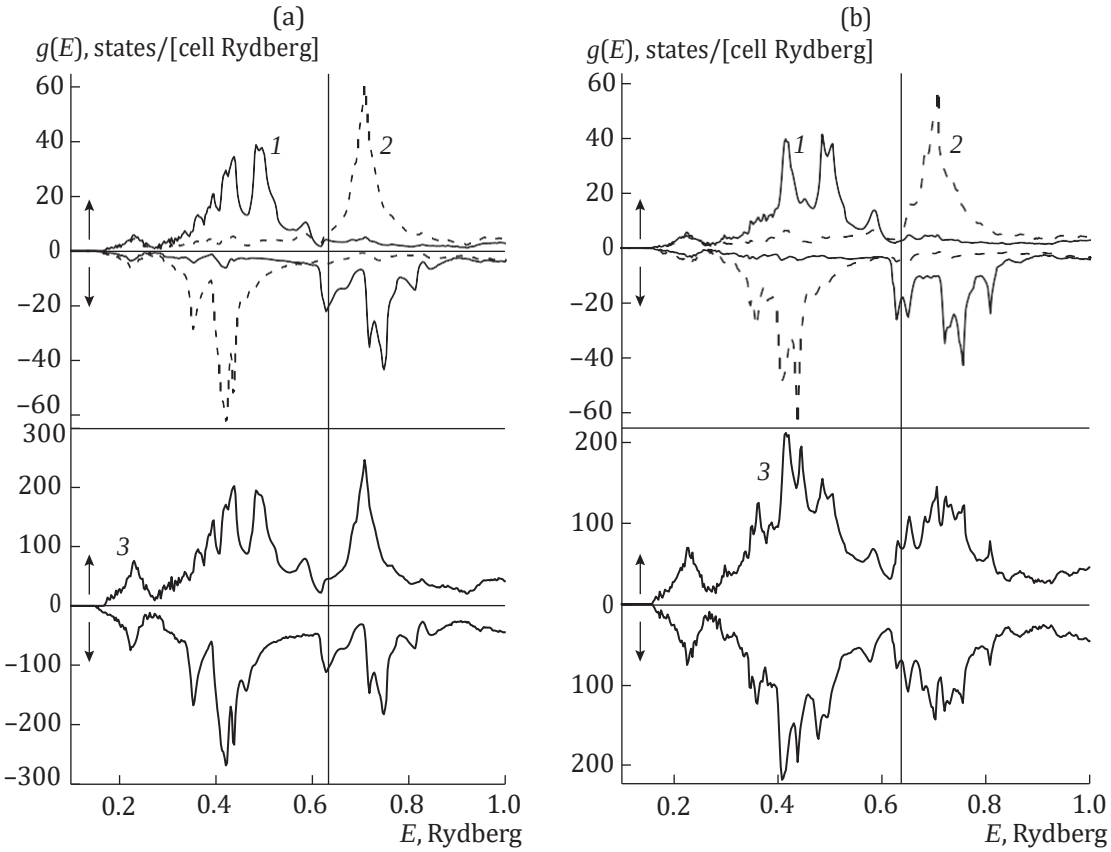

Fig. 3. Density of electronic states $g(E)$ to $Mn_{1.9}Cu_{0.1}Sb$ for ferrimagnetic (a) and antiferromagnetic (b) structures (curve (*1*) is the density of states of d-electrons Mn_I, (curve *2*) is the density of states of d-electrons of Mn_{II}, (curve *3*) is the total density of states); the vertical line indicates the position of the Fermi level.

vicinity of the Fermi level, which should significantly affect the interatomic exchange interactions of Mn_I–Mn_I in the alloy under consideration. Direct calculations of interatomic exchange integrals carried out for various magnetic structures confirm this assumption (Fig. 4, Table 1).

Table 1. Influence of Lattice Parameters and Type of Magnetic Structure on Interatomic Exchange Interactions J_{ij} for different values of parameters a and c

Structure	R_{ij}/a	J_{ij}, meV							
		a = 4.078 Å, c = 6.539 Å				a = 4.05 Å, c = 6.494 Å		a = 4.0 Å, c = 6.414 Å	
		FM	FIM	AF1	AF2	FIM	AF1	FIM	AF1
Mn_I–Mn_{II}	0.682	−11.9	5.6	5.1	−9.5	6.4	5.6	6.7	6.5
Mn_I–Mn_I	0.707	−21.9	−41.3	−19.5	−11.6	−36.9	−17.1	−31.2	−18.8
Mn_{II}–Mn_{II}	0.977	6.1	3.5	−0.5	−3.8	4.2	−0.8	6.3	−2.3
Mn_I–Mn_I	1.0	3.7	−2.0	−7.3	4.4	−2.2	−7.4	−1.5	7.5
Mn_{II}–Mn_{II}	1.0	6.2	6.0	7.2	3.6	5.9	7.3	5.9	−6.4
Mn_I–Mn_{II}	1.211	−4.3	4.7	3.6	−4.7	4.1	3.2	3.2	2.6
Mn_I–Mn_{II}	1.244	−4.3	6.0	−6.5	4.4	6.2	−7.0	6.2	−8.0
Mn_{II}–Mn_{II}	1.414	5.6	6.6	6.6	4.5	7.3	7.4	8.5	8.9
									−8.7*

Comparison of the total energies of magnetic structures for the main parameters of the crystal lattice (a = 4.078 Å, c = 6.539 Å) shows that the ground magnetic state is ferrimagnetic (FIM), and the remaining states lie higher in energy by 90 (FM), 134 (AF1) and 779 meV (AF2), respectively (Table 1.). * At high compression in the AF1 structure, a "splitting" of the exchange interaction Mn_{II}–Mn_{II}, which is a sign of the non-Heisenberg dependence of the exchange on the mutual orientation of the spins.

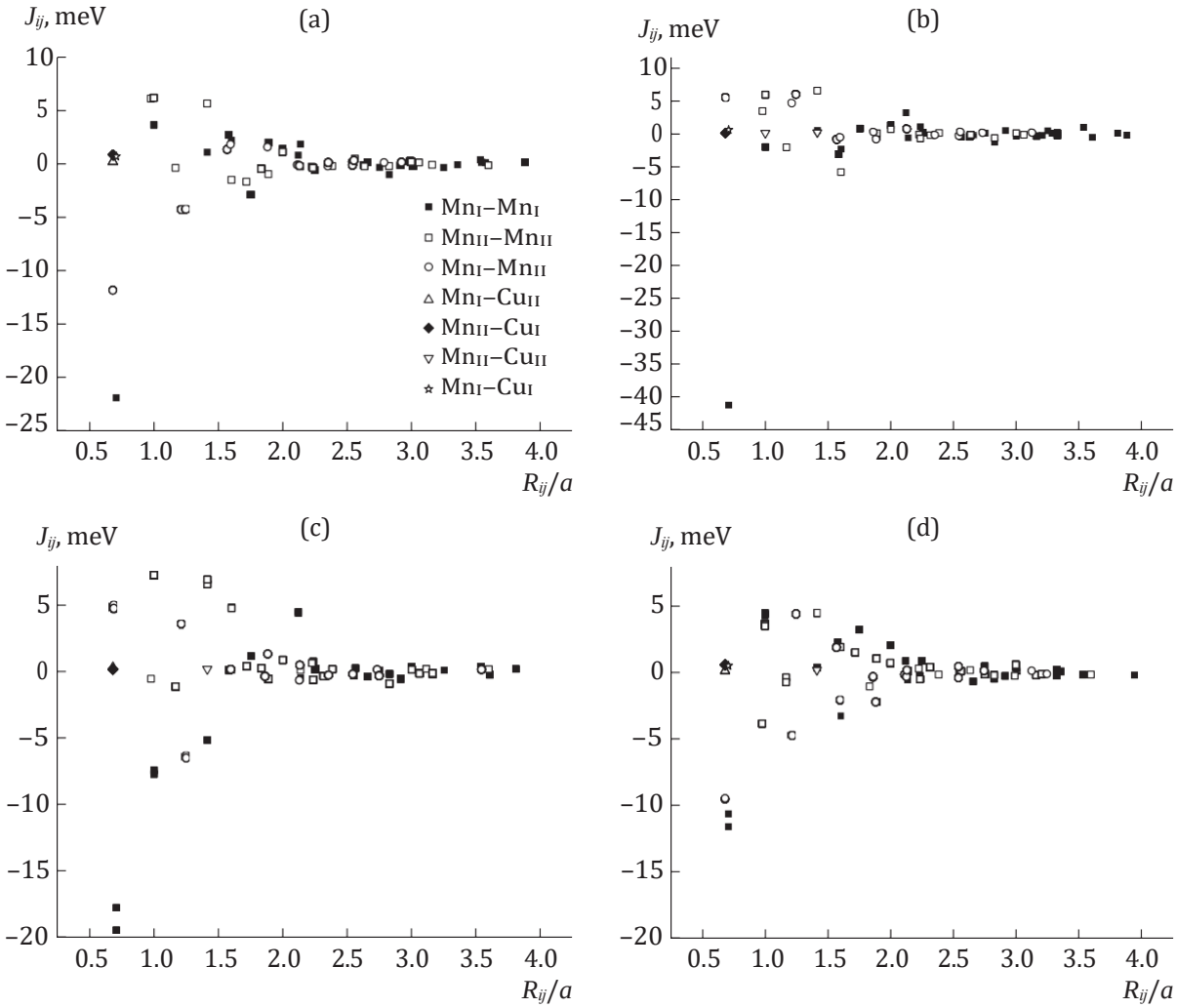

Fig. 4. Dependence of interatomic exchange integrals J_{ij} to $Mn_{1.9}Cu_{0.1}Sb$ from distance R_{ij}/a for the considered magnetic structures: FM (a), FIM (b), AF1 (c), and AF2 (d).

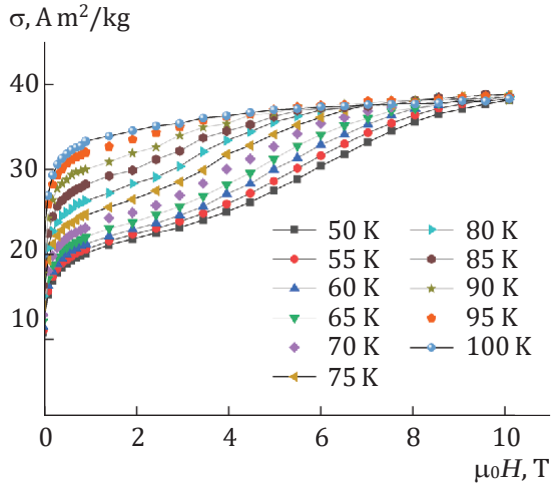

Fig. 5. Field dependences of magnetization of $Mn_{1.9}Cu_{0.1}Sb$ when the magnetic field induction changes from 0 to 10 T.

The magnetocaloric characteristics of the material under study were determined from a set of isothermal magnetization curves (Fig. 5) through Maxwell relation

$$\frac{\partial S}{\partial B} = \frac{\partial M}{\partial T}.$$

The temperature dependence of the change in magnetic entropy in the $Mn_{1.9}Cu_{0.1}Sb$ alloy determined in this way is shown in Fig. 6. The maximum value of the change in magnetic entropy is observed at a temperature of ~70 K.

As a result of the studies, it was found that when the magnetic field changes from 0 to 10 T the maximum magnetic entropy change for $Mn_{1.9}Cu_{0.1}Sb$ alloy is ~2 J/(kg K).

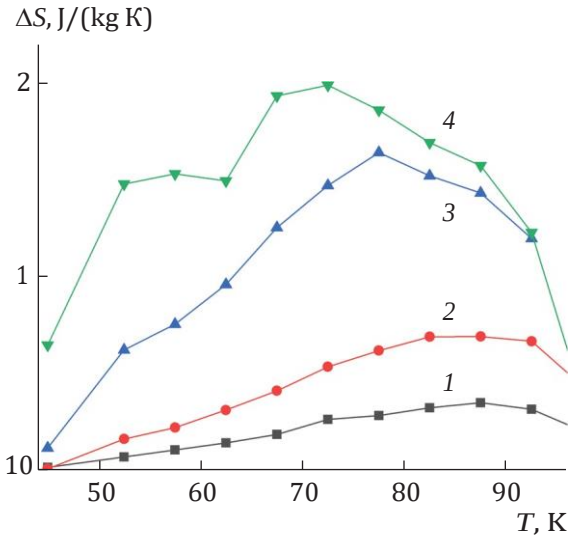

Fig. 6. The dependence of the change in magnetic entropy in the $Mn_{1.9}Cu_{0.1}Sb$ alloy at various magnetic fields: ΔIN = 0–1 (*1*), 0–2 (*2*), 0–5 (*3*), 0–10 T (*4*).

CONCLUSIONS

As a result of experimental studies, the presence of a relatively sharp decrease in the magnetization in the region of 100 K was established, which, according to the performed first-principles calculations, can be interpreted as antiferromagnetism–ferrimagnetism transitions.

The presence of a magnetic phase transition from a ferrimagnetic to an antiferromagnetic state (F ↔ AF) leads to the appearance of an inverse magnetocaloric effect, which, unlike several other compounds [15], is preserved in magnetic fields up to 10 T, which makes it promising to use $Mn_{1.9}Cu_{0.1}Sb$ as a working fluid for magnetic refrigerators.

FUNDING

This study was supported by the Belarusian Republican Foundation for Basic Research (project no. T20R-204) and the Russian Foundation for Basic Research (project no. 20-58-00059).

CONFLICT OF INTEREST

The authors declare that they do not have any conflicts of interest.

SPELL: 1. ok

REFERENCES

1. Q. Shen, I. Batashev, F. Zhang, et al., J. Alloys Compound **866**, Article No. 158963 (2021). https://doi.org/10.1016/j.jallcom.2021.158963
2. H. Zhang, R. Gimaev, B. Kovalev, et al., Physica B: Cond. Matt. **558**, 65 (2019). https://doi.org/10.1016/j.physb.2019.01.035
3. V. M. Ryzhkovskii, Metally, No. 3, 59 (2001).
4. Y. Q. Zhang, Z. D. Zhang, D. K. Xiong, et al., J. Appl. Phys. **94**, 4726 (2003). https://doi.org/10.1063/1.1608468
5. Y. Matsumoto, H. Orihashi, K. Matsubayashi, et al., IEEE Trans. Magn. **50** (1), Pt. 1, Article No. 1000704 (2014). https://doi.org/10.1109/TMAG.2013.2279536
6. Y. Matsumoto, K. Matsubayashi, Y. Uwatoko, et al., AIP Conf. Proc. **1763**, 020005 (2015). https://doi.org/10.1063/1.4961338
7. N. Yu. Pankratov, V. I. Mitsiuk, V. M. Ryzhkovskii, and S. A. Nikitin, J. Magn. Magn. Mater. **470**, 46 (2019). https://doi.org/10.1016/j.jmmm.2018.06.035
8. J. D. Wolf and J. E. Hanlon, J. Appl. Phys. **32** (12), 2584 (1961). https://doi.org/10.1063/1.1728358
9. V. I. Mityuk, G. S. Rimskii, V. V. Koledov, et al., Fiz. Tverd. Tela (St. Petersburg) **63**, 2082 (2021). https://doi.org/10.21883/FTT.2021.12.51669.153-2
10. H. Ebert, D. Kodderitzsch, and J. Minar, *J. Munich SPRKKR Package*, *Version 8.6*. (Ludwig-Maximilians Universitat, Munchen, 2010). www.ebert.cup.uni-muenchen.de/sprkkr.
11. H. Ebert, D. Kodderitzsch, and J. Minar, Rep. Prog. Phys. **74**, Article No. 096501 (2011).
12. S. H. Vosko and L. Wilk, Phys. Rev. B **22** (8), 3812 (1980). https://doi.org/10.1103/PhysRevB.22.3812
13. A. I. Liechtenstein, M. I. Katsnelson, V. P. Antropov, and V. A. Gubanov, J. Magn. Magn. Mater. **67**, 65 (1987). https://doi.org/10.1016/0304-8853(87)90721-9
14. V. N. Val'kov and A. V. Golovchan, Fiz. Nizk. Temp. **34** (1), 53 (2008).
15. K. A. Korolev, A. P. Sivchenko, I. F. Gribanov, et al., Celyab. Fiz.-Mat. Zh. **5** (4), 569 (2020). https://doi.org/10.47475/2500-0101-2020-15416
16. V. M. Rytskovskii, V. P. Glazkov, V. S. Goncharov, et al., Phys. Solid State **44**, 2281 (2002).